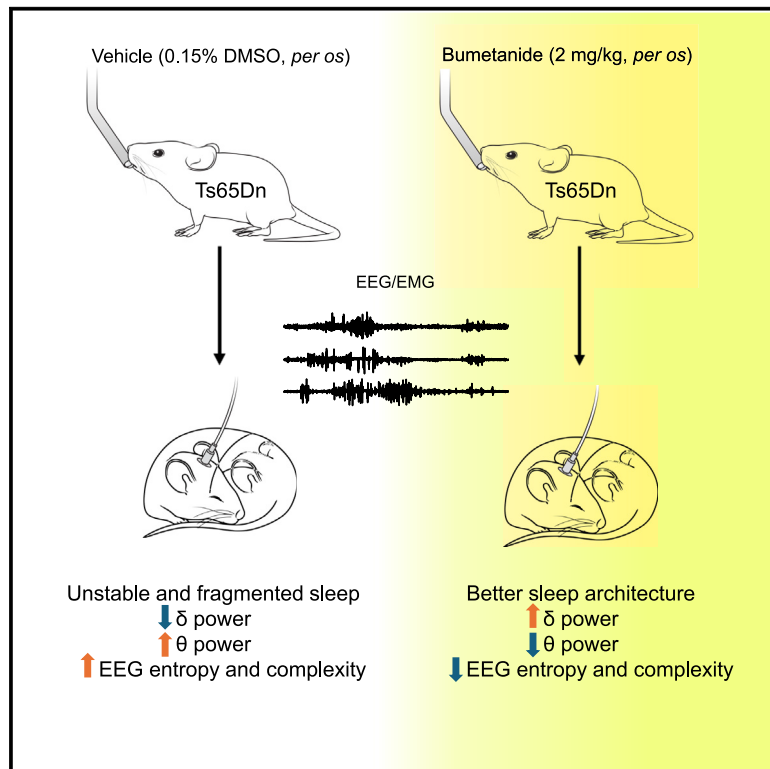


# NKCC1 inhibition improves sleep quality and EEG information content in a Down syndrome mouse model

## Graphical abstract



## Authors

Maria Bolla, Giulia Colombo, Matteo Falappa, ..., Fernando Montani, Valter Tucci, Laura Cancedda

## Correspondence

valter.tucci@iit.it (V.T.),  
laura.cancedda@iit.it (L.C.)

## In brief

Molecular biology; Neuroscience

## Highlights

- Ts65Dn mice show sleep instability and fragmentation, lower delta, and greater theta EEG power
- Bumetanide treatment improves sleep architecture, power spectrum and information content in Ts65Dn mice



## Article

# NKCC1 inhibition improves sleep quality and EEG information content in a Down syndrome mouse model

Maria Bolla,<sup>1,2,8</sup> Giulia Colombo,<sup>1,8</sup> Matteo Falappa,<sup>2,3,8</sup> Marta Pace,<sup>3</sup> Roman Baravalle,<sup>4,5</sup> Nataniel Martinez,<sup>6</sup> Fernando Montani,<sup>4</sup> Valter Tucci,<sup>3,9,\*</sup> and Laura Cancedda<sup>1,7,9,10,\*</sup>

<sup>1</sup>Brain Development and Disease Laboratory, Istituto Italiano di Tecnologia, Via Morego, 30, 16163 Genoa, Italy

<sup>2</sup>Università Degli Studi di Genova, Via Balbi, 5, 16126 Genoa, Italy

<sup>3</sup>Genetics and Epigenetics of Behavior Laboratory, Istituto Italiano di Tecnologia, Genoa, Italy

<sup>4</sup>Instituto de Física de La Plata (IFLP), CONICET-UNLP, La Plata, Buenos Aires, Argentina

<sup>5</sup>State University of New York (SUNY) Downstate Health Sciences University, Brooklyn, NY 11203, USA

<sup>6</sup>FIMAR (CONICET), Facultad de Ciencias Exactas y Naturales, Universidad Nacional de Mar Del Plata, B7602AYL, Mar Del Plata, Argentina

<sup>7</sup>Dulbecco Telethon Institute, Rome, Italy

<sup>8</sup>These authors contributed equally

<sup>9</sup>Senior authors

<sup>10</sup>Lead contact

\*Correspondence: [valter.tucci@iit.it](mailto:valter.tucci@iit.it) (V.T.), [laura.cancedda@iit.it](mailto:laura.cancedda@iit.it) (L.C.)

<https://doi.org/10.1016/j.isci.2025.112220>

## SUMMARY

In several brain disorders, the hyperpolarizing/inhibitory effects of GABA signaling through Cl<sup>-</sup>-permeable GABA<sub>A</sub> receptors are compromised, leading to an imbalance between neuronal excitation and inhibition. For example, the Ts65Dn mouse model of Down syndrome (DS) exhibits increased expression of the Cl<sup>-</sup> importer NKCC1, leading to depolarizing gamma aminobutyric acid (GABA) signaling in the mature hippocampus and cortex. Inhibiting NKCC1 with the Food and Drug Administration (FDA)-approved diuretic bumetanide rescues inhibitory GABAergic transmission, synaptic plasticity, and cognitive functions in adult Ts65Dn mice.

Given that DS individuals and Ts65Dn mice show sleep disturbances, and considering the key role of GABAergic transmission in sleep, we investigated whether NKCC1 upregulation contributes to sleep abnormalities in adult Ts65Dn mice. Chronic oral administration of bumetanide ameliorated the spectral profile of sleep, sleep architecture, and electroencephalogram (EEG) entropy/complexity, accompanied by a lower hyperactivity in trisomic mice. These results offer a potential avenue for addressing common sleep disturbances in DS.

## INTRODUCTION

Down syndrome (DS) is a genetic disorder characterized by developmental abnormalities arising from an additional copy of chromosome 21 in humans. The primary features of DS include intellectual disability and congenital birth defects.<sup>1</sup> Moreover, individuals with DS often experience other health issues, including sleep disorders.<sup>2</sup> These sleep disorders negatively impact the quality of life of both individuals with DS and their families, with up to 66% of adults with DS facing this burden. Obstructive sleep apnea (OSA) is prevalent in individuals with DS because of their unique craniofacial profile, weight, and upper airway muscle tone.<sup>3</sup> However, other electroencephalogram (EEG) abnormalities that are unrelated to OSA in DS individuals<sup>3</sup> and that compromise the entire architecture of sleep and wake have been reported. For example, individuals with DS often exhibit low-quality (deviations in NREM power spectral density) sleep and increased fragmentation (short and more frequent bouts in rapid eye movement [REM] and/or non-REM [NREM] sleep), as

well as reduced REM sleep.<sup>4–7</sup> Adolescents and young adults with DS present with a peculiar EEG power spectrum, which is characterized by reduced power density in the alpha band during waking; lower sigma power; reduced slow-wave activity in NREM sleep; and greater power in the delta, theta, and beta bands in waking and REM sleep.<sup>8–10</sup>

In DS mouse models (i.e., Ts65Dn, Ts1Cje, and Tc1 mice and partially in Dp(16)1Yey/+ mice<sup>11</sup>), a few experimental reports suggest a disruption in rest activity patterns, hyperactivity episodes, sleep fragmentation, and delayed sleep rebound after sleep deprivation (SD).<sup>12,13</sup> In particular, Ts65Dn mice show increased wakefulness at the expense of NREM, a reduced low-frequency range of the EEG power spectra (including delta power), and an increase in theta power.<sup>12</sup> Overall, mouse mutants mimicking human DS feature intrusions of wakefulness into sleep. Therefore, a potential treatment for restoring physiological sleep in DS should aim to increase overall sleep quality by restoring power spectral densities throughout the architecture of sleep stages (REM and NREM sleep).



Proper sleep maintenance is influenced by GABAergic transmission through  $\text{Cl}^-$  permeable GABA<sub>A</sub> receptors, as supported by research conducted in mice.<sup>14,15</sup> Moreover, wakefulness leads to a gradual change in  $\text{Cl}^-$  homeostasis and consequent variation toward depolarization in the  $\text{Cl}^-$  reversal potential through GABA<sub>A</sub> receptors in cortical pyramidal neurons owing to increased expression and activity of the Na-K- $\text{Cl}^-$  cotransporter 1 NKCC1.<sup>16</sup> This functional shift in the  $\text{Cl}^-$  reversal potential serves as the basis for electrophysiological and behavioral indicators of local sleep pressure, including NREM slow-wave activity levels, and low-frequency activity accompanied by decreased performance levels in cases of sleep deprivation.<sup>16</sup>

Research focused on cognitive impairment in Ts65Dn mice has highlighted defective GABAergic transmission, with particular emphasis on GABA<sub>A</sub>R-mediated signaling as a key player.<sup>17,18</sup> Among the diverse causes of defective GABA<sub>A</sub> signaling in DS mice, increased NKCC1 expression has been directly linked to poor cognitive outcomes.<sup>19</sup> Accordingly, chronic treatment of adult Ts65Dn mice with the NKCC1 inhibitors bumetanide [Food and Drug Administration (FDA)-approved diuretic, 3-(butylamino)-4-phenoxy-5-sulfamoylbenzoic acid] or ARN 23746 [3-(N,N-dimethylsulfamoyl)-4-((8,8,8-trifluorooctyl) amino)benzoic acid] and ARN 24092 [5-(N,N-dimethylsulfamoyl)-2-hydroxy-4-((8,8,8-trifluorooctyl)amino)benzoic acid] rescued their cognitive impairment.<sup>17,20–23</sup> Notably, bumetanide treatment was also able to rescue diverse core symptoms in other mouse models of diverse brain disorders (i.e., autism, Rett syndrome, fragile X syndrome, schizophrenia, traumatic brain injury, and epilepsy), which are all characterized by aberrant expression of  $\text{Cl}^-$  transporters and sleep impairment.<sup>22,24–27</sup>

Despite the vast involvement of GABA<sub>A</sub>ergic transmission in sleep and the role of  $\text{Cl}^-$  homeostasis in a large number of brain disorders, no systematic investigation has been conducted to determine whether bumetanide or other NKCC1 inhibitors ameliorate sleep disorder comorbidities associated with these brain disorders. Here, we found that chronic oral administration of bumetanide positively affected the spectral profile of sleep, partially affected sleep architecture and EEG entropy/complexity (as analyzed via different levels of detail and mathematical methods), and reduced hyperactivity in adult Ts65Dn mice. Other physiological behaviors, such as increased food intake, were not altered by the treatment, indicating a significant level of specificity of bumetanide for physiological sleep. Our findings suggest that impaired  $\text{Cl}^-$  homeostasis is involved in sleep disturbances in DS mice and suggest bumetanide as a potential therapy for improving sleep quality in DS.

## RESULTS

### Bumetanide treatment improves sleep architecture and power spectral density in Ts65Dn mice

To investigate the role of impaired  $\text{Cl}^-$  homeostasis in sleep in DS mice, we implanted wireless devices and measured EEG and electromyography (EMG) signals in adult (3–4 months; [Figure 1A](#)) Ts65Dn mice and their control wild-type (WT) littermates. Three days after surgery, the implanted mice were subjected to chronic treatment with bumetanide (2 mg/kg in drinking water)<sup>28</sup> or vehicle (0.15% DMSO in the drinking water) for four days

([Figures 1A and 2A](#)). On the fourth day of treatment, we conducted baseline EEG/EMG recordings over a 24-h period. At the beginning of the fifth day of treatment, we induced a 6-h sleep deprivation and then recorded it for an additional 18 h ([Figures 1A and 2A](#)). For data analysis, we segmented the EEG/EMG traces into 4-s epochs and then categorized the epochs into wakefulness, NREM sleep, or REM sleep epochs on the basis of their spectral features and mouse muscular activity. Consistent with prior studies,<sup>12</sup> our 24-h baseline EEG recordings revealed a tendency toward reduced total sleep duration in Ts65Dn mice compared with WT mice treated with vehicle (Ts Veh and WT Veh, respectively; [Figures 1B and S1A bottom](#), baseline). In the examination of typical sleep rebound after SD during the light phase (which corresponds to the sleep time of nocturnal animals such as mice), Ts Veh animals did not significantly differ from controls during the recovery phase ([Figures 1B and S1A bottom](#), recovery). Bumetanide treatment did not affect the total amount of sleep in Ts65Dn mice ([Figure S1A, top](#)), nor did it significantly affect sleep rebound in either experimental group ([Figure S1A, bottom](#)), implying that the increase in sleep pressure is not altered in Ts65Dn mice. Data on wakefulness duration and the percentage of wakefulness over the total recording time revealed a complimentary phenotype (vs. total sleep) for the vehicle-treated mice (wake, [Figure S1B](#)) at baseline and during recovery from SD. The amount of wakefulness upon bumetanide treatment slightly increased in Ts65Dn mice, but the main effect remained largely attributable to the genotype ([Figure S1B, top right](#)).

Although we found an unchanged overall amount of sleep in Ts65Dn mice compared with WT mice, when we performed an in-depth analysis of the sleep structure ([Table S1](#)), we discovered a reduction in NREM sleep duration during the light phase at baseline and after SD ([Figure 1C, left](#)), the percentage of NREM sleep over the total recording time after SD, and the percentage of NREM sleep over the total sleep time at baseline in Ts Veh compared with WT Veh mice ([Figure S1C](#)). Bumetanide treatment did not affect any of these parameters ([Figure 2B, left; Figure S1C](#)). Notably, we observed a significant increase in the REM sleep duration percentage over total sleep and a tendency to increase the REM sleep duration percentage over the total recording time ([Figure S1D](#)), with no significant changes in REM sleep duration in Ts65Dn compared with WT animals both during the baseline and after SD ([Figure 1D, left](#)). Additionally, for REM sleep duration, we detected no effect on either the Ts65Dn group or the WT group after bumetanide treatment ([Figure 2C, left; Figure S1D](#)).

Next, we analyzed sleep architecture ([Table S1](#)). The wake mean bout number over the whole recording time decreased in Ts65Dn mice, with no change in duration ([Figure S2A, top and bottom](#)). Notably, bumetanide treatment decreased the number of wake bouts in WT mice and increased the duration of wake bouts in both WT and Ts mice ([Figure S2A, bottom](#)). The number and duration of sleep bouts ([Figure S2B, top and bottom](#)) were significantly lower in Ts Veh than in WT Veh during total sleep, indicating greater instability and thus fragmentation of sleep. However, bumetanide treatment did not alter these phenotypes in Ts65Dn mice ([Figure S2B, right](#)) but decreased the number of sleep bouts in WT mice ([Figure S2B, middle top](#)).

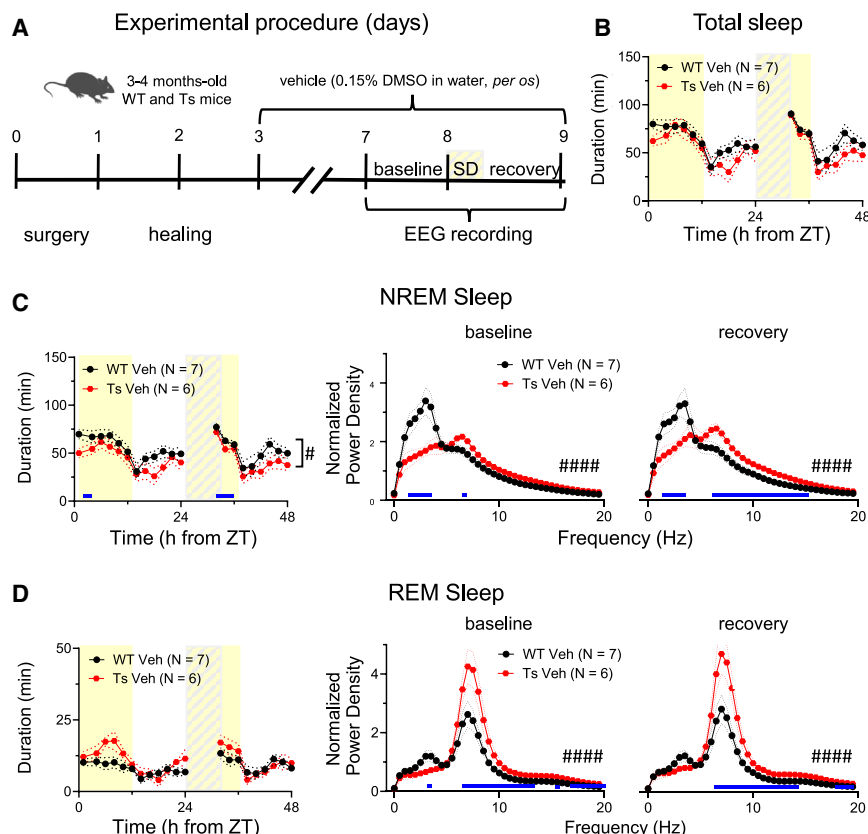


**Figure 1. Sleep structure and power spectral density are altered in the Ts65Dn mouse model of Down syndrome**

(A) Scheme of the experimental procedure with surgery, healing period (2 days), pharmacological treatment, and *in vivo* EEG recordings during baseline (24 h) and recovery (18 h) after sleep deprivation (6 h, SD) in adult mice.

(B) Quantification of the mean ( $\pm$ SEM) sleep duration across all recording period, binned every 2 h (WT Veh vs. Ts Veh, two-way ANOVA,  $F_{\text{genotype}}(1, 11) = 3.995$ ,  $p = 0.07$ ).

(C) (Left) Quantification of the mean ( $\pm$ SEM) NREM sleep duration in the same recordings in (B) (WT Veh vs. Ts Veh, two-way ANOVA,  $F_{\text{genotype}}(1, 11) = 7.371$ ,  $\#p < 0.05$ ; blue line indicates  $\#p < 0.05$  in *post hoc* Sidák's multiple comparison test). (Middle, right) Quantification of the mean ( $\pm$ SEM) EEG power densities over the frequency spectrum ( $\mu\text{V}^2/\text{Hz}$ ) during NREM sleep at baseline (middle, baseline: WT Veh vs. Ts Veh, two-way ANOVA,  $F_{\text{frequency band} \times \text{genotype}}(39, 429) = 7.162$ ,  $####p < 0.0001$ ; blue line indicates  $\#p < 0.05$  in *post hoc* Sidák's multiple comparison test) and after SD (right, recovery: WT Veh vs. Ts Veh, two-way ANOVA,  $F_{\text{frequency band} \times \text{genotype}}(39, 429) = 5.992$ ,  $####p < 0.0001$ ; blue line indicates  $\#p < 0.05$  in *post hoc* Sidák's multiple comparison test).

(D) (Left) Quantification of the mean ( $\pm$ SEM) REM sleep duration in the same recordings in (B) (WT Veh vs. Ts Veh, two-way ANOVA,  $F_{\text{genotype}}(1, 11) = 1.67$ ,  $p = 1.558$ ). (Middle, right) Quantification of the mean ( $\pm$ SEM) EEG power densities all over

the frequency spectrum ( $\mu\text{V}^2/\text{Hz}$ ) during REM at baseline (middle, baseline: WT Veh vs. Ts Veh, two-way ANOVA,  $F_{\text{frequency band} \times \text{genotype}}(39, 429) = 5.264$ ,  $####p < 0.0001$ ; blue line indicates  $\#p < 0.05$  in *post hoc* Sidák's multiple comparison test) and after SD (right, recovery: WT Veh vs. Ts Veh, two-way ANOVA,  $F_{\text{frequency band} \times \text{genotype}}(39, 429) = 4.776$ ,  $####p < 0.0001$ ; blue line indicates  $\#p < 0.05$  in *post hoc* Sidák's multiple comparison test). In all relevant panels, h from ZT: hours from the beginning of the recording (*zeitgeber*). Yellow represents the light phase, which is sleep time for nocturnal mice; white represents the dark phase, the active period; yellow and gray oblique stripes represent sleep deprivation. N indicates the number of recorded mice.

The number and duration of NREM bouts (Figure S3A, top and bottom) were decreased in Ts Veh, with no significant bumetanide effect but rather a reduction in the number of NREM bouts in WT mice (Figure S3A, top). The REM bout number was greater in Ts Veh than in WT Veh mice (Figure S3B, top; no change in duration; Figure S3B, bottom), indicating greater fragmentation of REM sleep. Interestingly, bumetanide was able to rescue this phenotype (Figure S3B, right, top). Moreover, bumetanide reduced the REM bout number in WT mice (Figure S3B, middle, top) and reduced the REM bout duration in Ts65Dn mice (Figure S3B, right, bottom).

Next, we performed analyses of the spectral characteristics of the EEG recordings (at 24 h after baseline and 18 h after SD) to determine the underlying neuronal activity and spectral correlates of sleep quality (which is directly correlated with NREM delta power,<sup>4</sup>; Table S1). We compared the EEG power density for delta (0, 5–5 Hz)<sup>29</sup> and theta (5–10 Hz) waves<sup>30</sup> in the NREM and REM sleep phases, which are indicators of sleep depth/quality and hippocampal function, respectively.<sup>4,31</sup> As previously reported,<sup>12</sup> we detected a statistically significant reduction in delta power and an increase in theta power in Ts Veh mice compared with WT Veh mice both at baseline and dur-

ing recovery during NREM sleep (Figure 1C, middle and right). Notably, bumetanide treatment significantly rescued the power density of the delta and theta bands in Ts65Dn animals toward WT levels at baseline and during recovery (Figure 2B, middle and right).

Finally, when analyzing REM sleep, we again detected a decrease in the delta power density and an increase in the theta power density in Ts Veh compared with WT Veh at baseline (Figure 1D, middle), with an increase in theta power but a nonsignificant trend toward delta power at recovery (Figure 1D, right). Bumetanide treatment also significantly rescued the power spectral density of Ts Veh mice toward WT levels both before (Figure 2C, middle, bottom) and after SD (Figure 2C, recovery, right, bottom).

Bumetanide had no effect on the EEG power spectral density in WT animals (Figures 2B and 2C, middle and right, top).

Overall, several sleep features (instability and fragmentation, Table S1) were greater in Ts65Dn than in WT mice, with fewer and shorter NREM bouts and more REM bouts of the same average length, and these were partially ameliorated by bumetanide treatment. Bumetanide treatment particularly improved sleep quality (Table S1), with improvements in the power density of delta and theta waves in both the NREM and REM sleep

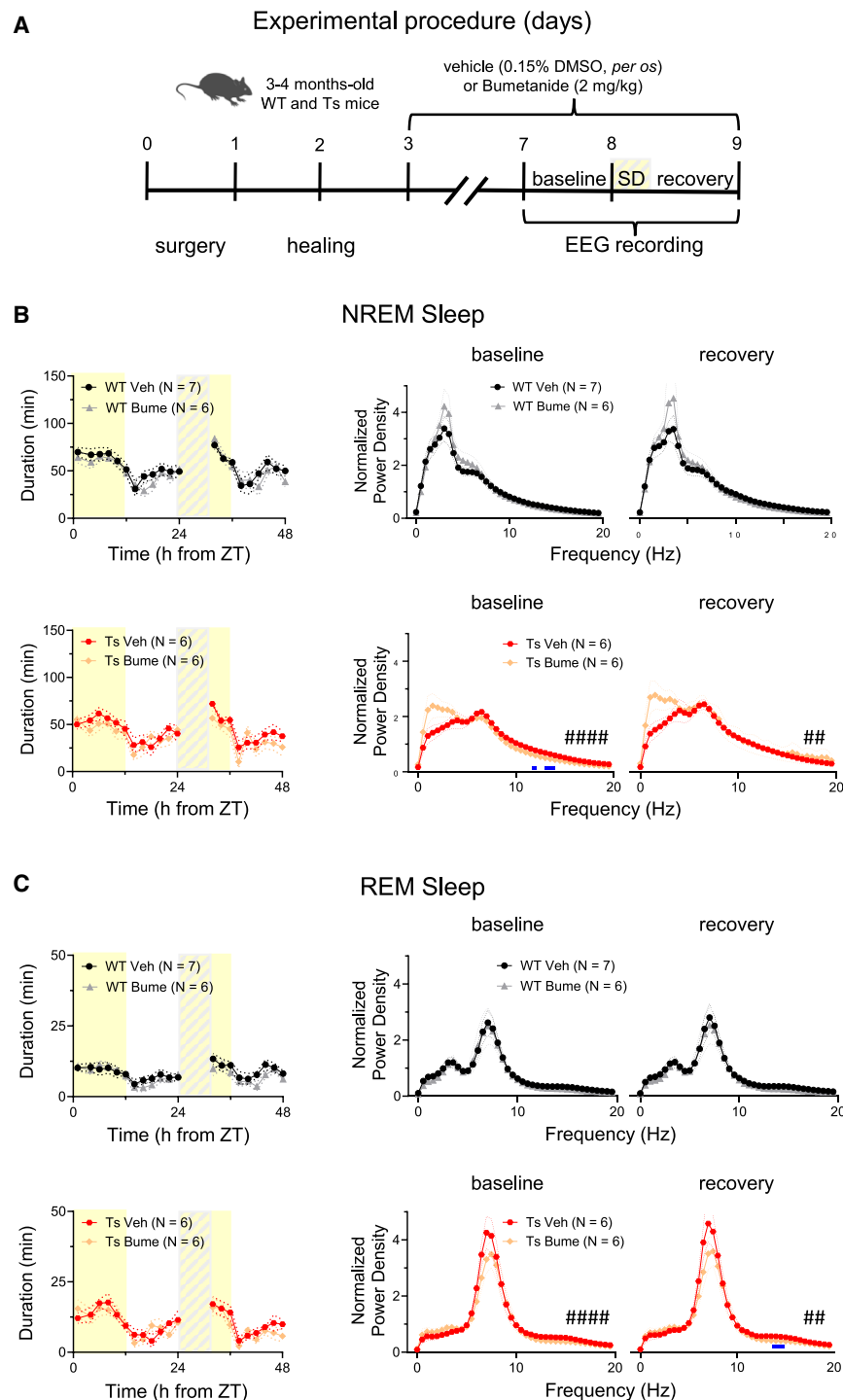


**Figure 2. Bumetanide significantly rescues power spectral density in adult Ts65Dn mice**

(A) Scheme of the experimental procedure with surgery, healing period (2 days), pharmacological treatment, and *in vivo* EEG recordings during baseline (24 h) and recovery (18 h) after sleep deprivation (6 h, SD) in adult mice.

(B) (Left) Quantification of the mean ( $\pm$ SEM) NREM sleep duration in the same set of experiments of Figure 1 with animals treated with Vehicle or bumetanide (WT Veh vs. WT Bume, two-way ANOVA,  $F_{\text{genotype}} (1, 11) = 0.7476$ ,  $p = 0.4057$ ; Ts Veh vs. Ts Bume, two-way ANOVA,  $F_{\text{genotype}} (1, 11) = 1.582$ ,  $p = 0.2371$ ). (Middle, right) Quantification of the mean  $\pm$  SEM EEG power densities over the frequency spectrum ( $\mu\text{V}^2/\text{Hz}$ ) during NREM sleep at baseline (middle, baseline: WT Veh vs. WT Bume, two-way ANOVA,  $F_{\text{frequency band} \times \text{genotype}} (39, 429) = 0.8013$ ,  $p = 0.7997$ ; Ts Veh vs. Ts Bume, two-way ANOVA,  $F_{\text{frequency band} \times \text{genotype}} (39, 390) = 2.642$ ,  $####p < 0.0001$ ; blue line indicates  $*p < 0.05$  in post hoc Sidák's multiple comparison test) and after SD (right, recovery: WT Veh vs. WT Bume, two-way ANOVA,  $F_{\text{frequency band} \times \text{genotype}} (39, 429) = 0.9621$ ,  $p = 0.5383$ ; Ts Veh vs. Ts Bume, two-way ANOVA,  $F_{\text{frequency band} \times \text{genotype}} (39, 390) = 1.921$ ,  $##p < 0.01$ ).

(C) (Left) Quantification of the mean ( $\pm$ SEM) REM sleep duration in the same set of experiments of Figure 1 with animals treated with Vehicle or bumetanide (WT Veh vs. WT Bume, two-way ANOVA,  $F_{\text{genotype}} (1, 11) = 0.7476$ ,  $p = 0.4057$ ; Ts Veh vs. Ts Bume, two-way ANOVA,  $F_{\text{genotype}} (1, 11) = 1.582$ ,  $p = 0.2371$ ). (Middle, right) Quantification of the mean ( $\pm$ SEM) EEG power densities over the frequency spectrum ( $\mu\text{V}^2/\text{Hz}$ ) during REM sleep at baseline (middle, baseline: WT Veh vs. WT Bume, two-way ANOVA,  $F_{\text{frequency band} \times \text{genotype}} (39, 429) = 0.8013$ ,  $p = 0.7997$ ; Ts Veh vs. Ts Bume, two-way ANOVA,  $F_{\text{frequency band} \times \text{genotype}} (39, 390) = 2.642$ ,  $####p < 0.0001$ ) and after SD (right, recovery: WT Veh vs. WT Bume, two-way ANOVA,  $F_{\text{frequency band} \times \text{genotype}} (39, 429) = 0.9621$ ,  $p = 0.5383$ ; Ts Veh vs. Ts Bume, two-way ANOVA,  $F_{\text{frequency band} \times \text{genotype}} (39, 390) = 1.921$ ,  $##p < 0.01$ ; blue line indicates  $*p < 0.05$  in post hoc Sidák's multiple comparison test). In all relevant panels, h from ZT: hours from the beginning of the recording (zeitgeber); the recording time was binned every 2 h. Yellow represents the light phase, which is sleep time for nocturnal mice; white represents the dark phase, the active period; yellow and gray oblique stripes represent sleep deprivation. N indicates the number of recorded mice.

phases before and after SD and no significant changes in WT animals. However, there was a wake-stabilizing effect.

### Bumetanide treatment reduces EEG entropy and complexity in Ts65Dn mice

EEG signals are time series that can be considered complex systems that are neither perfectly ordered nor completely disor-

dered but exhibit a certain degree of structure. Time-domain entropy and complexity measures can be highly sensitive to subtle abnormalities in brain activity that may not manifest in spectral analysis. For example, early stage neural disorders may show changes in the time-domain characteristics of signals that are more challenging to detect through traditional spectral methods. Estimating entropy and complexity in brain signals (like EEGs) in



the time domain offers insights that differ from those of traditional frequency-domain analysis. This provides a complementary perspective to spectral analysis.<sup>32–35</sup> If a specific arrangement of the main features that an EEG can express exists, it introduces structure, reducing disorder. Therefore, if the recorded EEG is in a state where everything is in its place, entropy—the “disorder”—and complexity are quite low. However, if EEG features are scattered and not in their expected arrangement, complexity and entropy increase (see [STAR Methods](#) for a full description).

To assess the information content and structure ([Table S1](#)) of the rhythmic oscillations in the EEG, we thus calculated the intrinsic correlational structure of the Ts65Dn and WT mouse EEG signals via entropy (H) and complexity (C) estimations. This mathematical approach, derived from information theory,<sup>32,36</sup> is represented by the causality plane  $H \times C$  ([Figure S4A](#)). First, we computed the time course of entropy and complexity for the whole-frequency EEG signal in both WT Veh and Ts Veh full-length recordings and found no differences in the general trend over time for wake, NREM, and REM recordings for the two mouse genotypes ([Figure S4B](#)). However, when we calculated entropy and complexity separately for each sleep stage (NREM and REM) and divided by frequency bands, we found that the mean delta band entropy and complexity values in NREM sleep were greater in Ts Veh than in WT Veh. This result indicates greater uncertainty in the signals in Ts Veh ([Figure S4C, left](#); [Figure 4D, left](#)), suggesting a defective orchestration of delta waves. Bumetanide treatment rescued Ts65Dn delta band entropy and complexity to WT levels, suggesting a potential role of  $Cl^-$  homeostasis in regulating the entropy and complexity of EEG signals ([Figures S4C and S4D, left](#)). Conversely, the mean theta band in REM sleep entropy values exhibited only a nonsignificant trend toward a reduction in Ts Veh vs. WT Veh, and bumetanide increased the values closer to WT levels ([Figures S4C and S4D, right](#)).

Thus, the delta frequency band entropy and complexity in NREM sleep were greater in trisomic mice than in control mice, and this alteration was reversed by bumetanide treatment. This finding is consistent with the rescue that we observed in power spectral density upon NKCC1 inhibition.

The higher entropy and complexity suggest more irregular signals with temporal correlation structure patterns of brain activity. These findings indicate greater unpredictability and more intricate temporal patterns in their brain activity. This reflects altered electrical activity, which could be related to neural connectivity or dysfunction in sleep-related regulatory mechanisms. The information theory metrics are presented in their normalized versions as a standard procedure, allowing for accurate comparisons across different datasets or conditions. Although the differences seem small, they are statistically significant.

### Bumetanide treatment decreases daily hyperactivity but has no effect on body temperature or increased food intake in Ts65Dn mice

Ts65Dn mice and people with DS exhibit hyperactivity.<sup>37,38</sup> We thus assessed motor activity in adult Ts65Dn mice and WT littermates treated with vehicle or bumetanide. To this end, we took advantage of the activity signal recorded by the wireless implant and monitored the mice over 48 h ([Figure 3A](#)). We found that Ts

Veh mice presented greater motor activity than WT Veh mice did at baseline during the light phase and presented an increasing trend during the dark phase ([Figure 3B, left](#)). Bumetanide treatment partially reversed this hyperactivity in Ts65Dn mice ([Figure 3B, left](#)). After SD, no significant increase in the activity of Ts Veh mice was noted during either the light or dark phase ([Figure 3B, right](#)). This effect was not altered by bumetanide treatment ([Figure 3B, right](#)).

Next, because the regulation of body temperature exerts control over sleep in mammals,<sup>39</sup> we also assessed the circadian profile of body temperature in adult Ts65Dn mice and WT littermates using our wireless EEG transmitter/receiver, which also contains a subcutaneous sensor to detect body temperature. We found no significant differences in body temperature between the WT Veh and Ts Veh mice throughout the recording time, before and after sleep deprivation, with an effect on the genotype during the dark phase at baseline ([Figure 3C](#)). Overall, bumetanide treatment had no effect on body temperature ([Figure 3C](#)).

Finally, we monitored the amount of food consumed over 24 h and detected a statistically significant increase in food intake in Ts Veh mice compared with WT Veh mice. Bumetanide had no effect on food intake behavior ([Figure 3D](#)).

Thus, bumetanide treatment decreased hyperactivity in Ts65Dn mice, but it had no effect on food intake or body temperature.

## DISCUSSION

Electrophysiological sleep, a complex brain state present across species, has been thoroughly characterized through the identification of stages and minimal electrophysiological features.<sup>40</sup> Previous efforts to compare sleep between mice and humans have yielded a rich repertoire of specific translational features.<sup>41</sup> This background served as a valuable foundation in the context of preclinical studies in DS.

Compared with those of WT mice, the sleep instability and fragmentation of Ts65Dn mice were greater, the delta power was lower, and the theta power was greater during both NREM and REM sleep, which is consistent with the literature on most other DS mouse models<sup>12,13</sup> (but see *Dp(16)1Yey/+<sup>11</sup>*). In addition, we also reported that trisomic mice presented with greater delta frequency entropy and complexity during NREM sleep, highlighting a difference in the EEG information content and signal structure between DS and WT mice. We did not analyze gamma rhythms in our study because our EEG/EMG recording system did not have sufficient sampling frequency or insulation from high-frequency environmental noise to achieve clean gamma power density extraction (see [STAR Methods](#)). However, despite the significant increase in theta power, we did not find significant differences in the entropy and complexity analyses within the theta band. This finding suggests that although the overall amplitude of theta oscillations (as reflected in power) is greater in trisomic mice, the underlying temporal organization and unpredictability (as measured by entropy) and the level of structural organization (as measured by complexity) remain comparable to those in WT mice.

In our work, we reported that rescue of brain  $Cl^-$  homeostasis by NKCC1 inhibition ameliorated some specific sleep features,

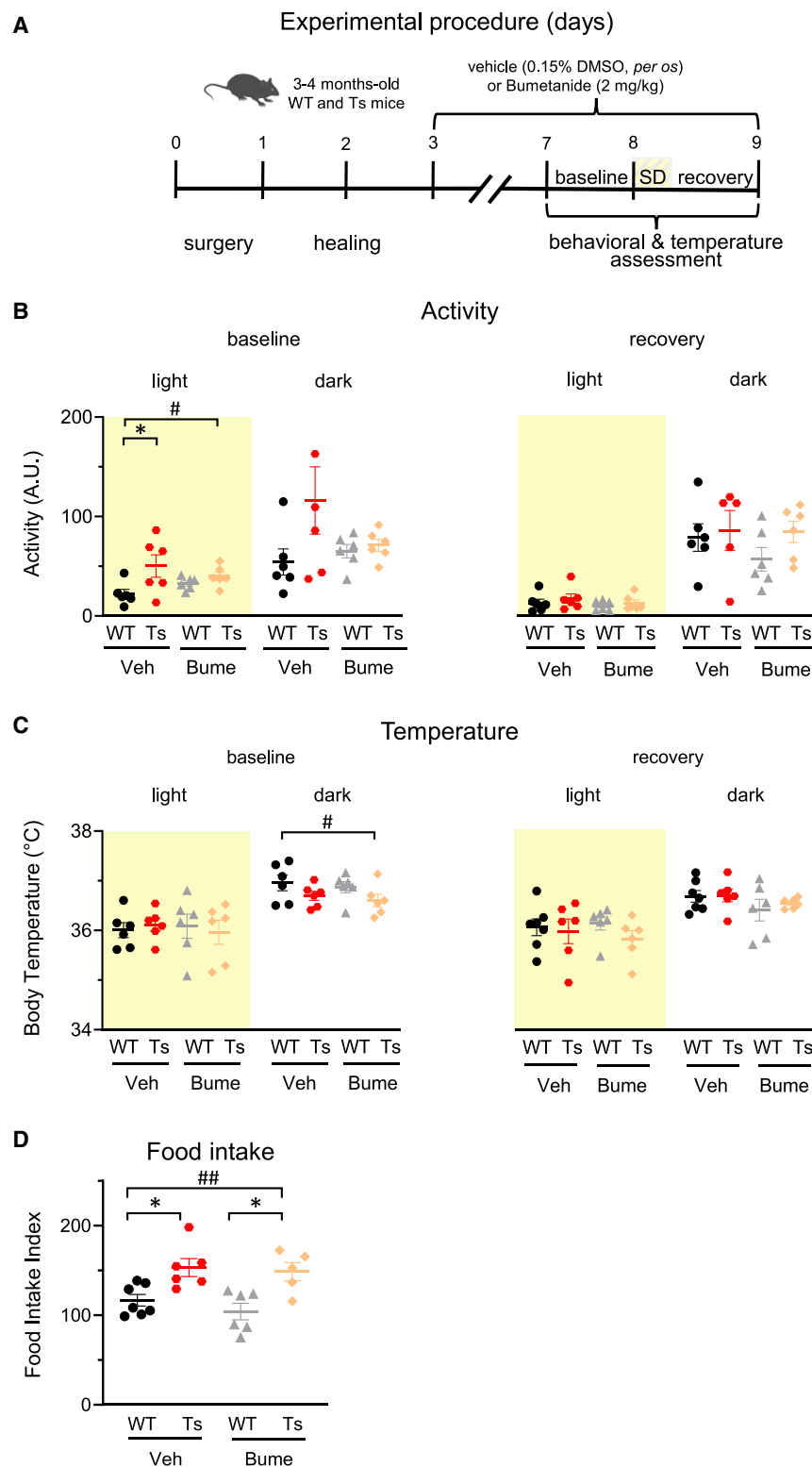


**Figure 3. Bumetanide partially rescues daily baseline hyperactivity, but it does not impact on body temperature or food intake in adult Ts65Dn mice**

(A) Scheme of the experimental procedure with surgery, healing period, pharmacological treatment, and assessment of activity behavior and body/temperature during baseline and recovery after SD. These experiments were performed on the same animals as for Figures 1 and 2.

(B) Quantification of the mean ( $\pm$ SEM) activity across 24 h at baseline (light, two-way ANOVA, Fgenotype (1, 20) = 7.37,  $\#p < 0.05$ ; dark, two-way ANOVA, Fgenotype (1, 20) = 3.27,  $p = 0.0856$ ;  $*p < 0.05$ , post hoc Sidák's multiple comparisons test) and 18 h after SD (recovery; light, two-way ANOVA, Fgenotype (1, 20) = 0.9379,  $p = 0.3444$ ; dark, two-way ANOVA, Fgenotype (1, 20) = 2.224,  $p = 0.1515$ ).

(C) Quantification of the mean ( $\pm$ SEM) body temperature across 24 h at baseline (light, two-way ANOVA, Fgenotype (1, 21) = 0.0763,  $p = 0.7851$ ; dark, two-way ANOVA, Fgenotype (1, 21) = 5.233,  $\#p < 0.05$ ) and 18 h after SD (light, two-way ANOVA, Fgenotype (1, 21) = 0.0411,  $p = 0.8413$ ; dark, two-way ANOVA, Fgenotype (1, 21) = 2.504,  $p = 0.1285$ ).

(D) Quantification of the mean ( $\pm$ SEM) food intake index (mg of food consumed in 24 h/g of mouse weight) across 24 h at baseline (one-way ANOVA with Welch correction, F(4,24) = 6.973,  $\#\#p < 0.01$ ; post hoc Dunnett's T3 multiple comparisons test,  $*p < 0.05$ ). For all graphs, each dot represents the value recorded for one mouse. Yellow represents the light phase, which is sleep time for nocturnal mice; white represents the dark phase, the active period.

which account for the quality of sleep and the entropy/complexity of EEG information. This finding indicates a potentially better ability of the neural network to correctly process information. In particular, we showed that bumetanide treatment rescued the power density of delta and theta waves in both the NREM and REM sleep phases before and after SD. Moreover, sleep architecture (instability and fragmentation) in terms of reduced sleep bout number was also rescued by bumetanide treatment. In WT animals, bumetanide also aided in decreasing the wake bout number and increasing the wake bout duration, thus affecting their wake microarchitecture and potentially sleep pressure build-up. Indeed, the chloride-current reversal potential gradually shifts from hyperpolarizing to depolarizing over the time spent awake,<sup>16</sup> which is positively correlated with the buildup of sleep pressure. In addition, bumetanide keeps the GABA<sub>A</sub>R reversal potential hyperpolarizing longer,<sup>42</sup> thus potentially counteracting sleep pressure buildup and increasing wake stability.

The entropy and complexity of the delta band in NREM sleep of Ts65Dn mice reached WT levels with bumetanide treatment, suggesting a recovery of the regularity of oscillations<sup>36</sup> potentially through a better synchrony of distributed oscillators in the brain<sup>43</sup> and delta rhythm generators. A similar effect occurred for REM sleep theta band entropy, which tended to decrease in Ts Veh mice, implying a greater efficiency of theta rhythm generators. This finding was consistent with the increase in theta power in Ts Veh mice. Moreover, bumetanide rescued theta band entropy to WT levels. Thus, bumetanide treatment has the potential to improve the quality of sleep by both ameliorating the delta power in NREM sleep and improving sleep architecture (rescue of REM bout number) in people with DS.

Although we found positive effects of bumetanide treatment on sleep quality and EEG information content in Ts65Dn, the rescue of the DS sleep phenotype observed here by NKCC1 inhibition was only partial compared with the WT levels. This finding was potentially observed because we could not increase the bumetanide dosage at optimal levels, as it would lead to excessive diuresis.<sup>23</sup> Moreover, our only partial rescue may also be a consequence of the restless behavior of mice given the need to constantly urinate after diuretic treatment.<sup>23</sup> Alternatively, the lack of total rescue of sleep patterns by our bumetanide treatment may be because we administered bumetanide to mice of an adult age, i.e., when the sleep-wake cycle and pattern had already fully developed and matured. Early intervention may better rescue the neurodevelopmental phenotype (including sleep disturbances) because sleep alterations have a strong developmental component and spectral alterations in individuals with DS are age dependent.<sup>44,45</sup> On the other hand, the positive effect of bumetanide treatment on sleep that we found in adult DS mice, even if only partial, supports the growing concept in the field of neurodevelopmental disorders, indicating that (at least some) clinical symptoms can still be rescued by pharmacological treatments at late stages of development and/or adulthood.

The neurological underpinnings of the rescue of the sleep power spectral density profile in Ts65Dn mice by systemic NKCC1 inhibition may be linked to the restoration of the imbalanced excitatory/inhibitory activity ratio in neurons of the septo-hippo-

campal pathway (which is the primary generator of theta rhythm in the brain<sup>46</sup>) and of the cortex (key structure of the delta oscillator together with the thalamus<sup>47</sup>). In fact, the increased EEG theta power observed in Ts65Dn mice may simply result from NKCC1 upregulation in the hippocampus and cortex.<sup>12,17</sup> Nevertheless, NKCC1 expression may also be deregulated in the septum, thalamus, or other oscillating neuronal networks known to participate in the delta and theta rhythms. Accordingly, blockage or potentiation of GABA<sub>A</sub> receptor signaling eliminates theta and delta rhythms in WT animals.<sup>47</sup>

NKCC1 is also highly expressed in glial cells such as oligodendrocytes,<sup>48</sup> ependymal cells,<sup>49</sup> and astrocytes.<sup>50</sup> In addition, sleep supports oligodendrocyte functions, such as lipid metabolism and myelination deposition, and promotes the proliferation of new immature oligodendrocytes.<sup>48,51</sup> Moreover, oligodendrocytic NKCC1 is involved in the induction of myelinated fiber plasticity via neuron-induced oligodendrocyte depolarization.<sup>52</sup> This form of fiber plasticity enhances hippocampal CA1-subiculum LTP, and NKCC1 knockdown reduces it in wild-type mice.<sup>52</sup> However, bumetanide treatment has been demonstrated to be effective in restoring CA3-CA1 LTP in Ts65Dn mice.<sup>42</sup> This finding highlights that the effect of neuronal NKCC1 inhibition, which rescues aberrantly depolarizing GABA, likely extends to oligodendrocytic NKCC1, leading to beneficial cognitive rescue in this mouse model of DS. Bumetanide has also been demonstrated to be effective in preventing white matter damage in a rat model of preterm brain injury, likely by blocking NKCC1 expressed by both neurons and oligodendrocytes<sup>48</sup> and confirming the importance of this transporter for the homeostasis of myelin. On the other hand, ependymal cells can secrete immunomodulators such as interleukin-18 (IL-18), which can influence sleep.<sup>53</sup> In addition, these cells highly express NKCC1 on the luminal side, which is a key player in cerebrospinal fluid (CSF) secretion<sup>49</sup>; however, the link between these two phenomena remains elusive. Bumetanide reduces NKCC1-dependent CSF secretion, which accounts for 50% of total CSF production. This effect has been demonstrated to be beneficial in hydrocephalus models, but it does not impact control animals.<sup>49</sup> Astrocytes exhibit dynamic activity across the sleep-wake cycle and may encode sleep need via changes in intracellular signaling pathways, including elevated calcium.<sup>54</sup> NKCC1 also regulates Cl homeostasis in astrocytes, contributing to regulating cell volume, proliferation, and apoptosis, as well as supporting inhibitory neurotransmission.<sup>50</sup> Bumetanide reduced calcium storage in the endoplasmic reticulum of astrocytes, but the consequences of this effect for sleep regulation remain unclear.<sup>55</sup>

Sleep disturbances may also be causally linked with the poor cognitive performance of people with DS.<sup>56</sup> Indeed, many studies have reported the important role of sleep in task acquisition and memory consolidation in humans and mice.<sup>57–59</sup> In particular, higher delta power in NREM sleep in humans correlates with better sleep quality,<sup>4</sup> contributes to the consolidation of memories, and restores executive function.<sup>60</sup> Moreover, insufficient delta power (as we found here in Ts65Dn mice) is linked to cognitive deficits in WT mice.<sup>18,61–65</sup> Interestingly, a reduction in NREM delta power is also linked to aging, Alzheimer disease, and Parkinson disease, all of which are associated with various



degrees of cognitive impairment.<sup>60,66,67</sup> Thus, the known rescue of cognitive impairment in Ts65Dn mice<sup>17</sup> by bumetanide treatment may also depend (at least in part) on its rescue of delta power in NREM sleep, as we report here.

In humans, during wakefulness, hippocampal theta oscillations support memory integration,<sup>68,69</sup> and theta activity in the frontal cortex is a marker of increased cognitive control demands.<sup>70,71</sup> Interestingly, EEG theta power is often increased in people with neurological diseases, such as Alzheimer disease<sup>72,73</sup> and Parkinson disease.<sup>74</sup> Moreover, in mice, variations in the peak of theta power during diverse sleep stages have many cognitive correlates (e.g., offline memory processing, memory consolidation, spatial location encoding, emotional memory, and memory plasticity<sup>75–77</sup>). Finally, abnormal theta synchronicity has been found in the hippocampus of Ts65Dn mice, particularly in interneurons,<sup>78</sup> and GABAergic interneurons play a key role in underlying synchronizing events in WT mice.<sup>79</sup> Thus, this evidence on theta power and cognition from the literature together with the alteration in theta power reported in this study using Ts65Dn mice indicate a possible causal relationship among network theta synchronization and memory, as well as interneuron function and chloride homeostasis.

Finally, sleep disturbances may also be implicated in the well-known clinical evolution of people with DS toward early dementia (Alzheimer disease).<sup>12,80</sup> Indeed, sleep disturbances are often associated with a greater risk of cognitive decline or dementia<sup>81</sup> and are early signs of Alzheimer disease, which is likely linked to its pathogenesis.<sup>82,83</sup>

From this general perspective, pharmacological therapy aimed at improving sleep quality via NKCC1 inhibition could also indirectly benefit cognitive performance. Interestingly, a phase II clinical trial (EudraCT Number: 2015-005780-16) is currently ongoing to evaluate bumetanide repositioning to treat cognitive impairment in people with DS, and its exploratory endpoints also include questionnaires for sleep feature assessment. If successful, this study will set the groundwork for a phase III trial including sleep rescue among secondary outcomes or future phase II clinical trials with sleep rescue as a primary endpoint.

An increase in motor activity is a well-documented behavioral characteristic in individuals with DS and diverse DS mouse models,<sup>84,85</sup> as we also found here in Ts65Dn mice. Hyperactivity is linked to behavioral arousal and to the neuromodulatory state underlying the sleep-wake circadian rhythm.<sup>86,87</sup> Interestingly, attention-deficit hyperactive disorder (ADHD) is more common in individuals with DS than in the general population,<sup>84</sup> and sleep disturbances have been associated with hyperactivity in children with ADHD.<sup>88,89</sup> Using Ts65Dn mice, we found results similar to that reported in the literature.<sup>17,19</sup> These results demonstrate that hyperactivity manifests as an increase in exploratory behavior during the dark and light periods compared with controls. Interestingly, although we found here that bumetanide treatment reduced motor activity in adult Ts65Dn mice, bumetanide treatment or downregulation of NKCC1 expression in the hippocampus was ineffective in two other studies.<sup>17,19</sup> This difference may be attributed to different experimental conditions. The literature studies utilized an array of photocell beams to count mouse transitions over a period of 24 h or evaluated motor activity as a correlate of the distance traveled in 15 min by

mice in an empty arena, whereas our study employed implants to continuously monitor mouse movements over 48 h. Thus, our study allowed for a better sampling of the activity, similar to what happens in human actigraphy.<sup>90</sup> Moreover, in our study, we systemically administered bumetanide in the drinking water for sustained NKCC1 inhibition throughout the day and in all brain regions. Conversely, in the first study from the literature, bumetanide treatment was administered by intraperitoneal injection.<sup>20</sup> Given bumetanide's short half-life,<sup>22</sup> this may have not guaranteed sustained NKCC1 inhibition over time. On the other hand, in the second study from the literature, NKCC1 knock-down was long-lasting but limited to the hippocampal region, so it likely had a smaller effect on locomotor function, which depends on brain regions other than the hippocampus.

The regulation of body temperature and sleep are closely linked in mammals.<sup>91</sup> However, under our experimental conditions, we observed only a minor difference in body temperature between Ts65Dn and WT mice. On the other hand, we found that the reduced sleep in Ts65Dn mice was accompanied by increased food intake, consistent with the findings of a recent study<sup>92</sup> and that people with DS often have an insatiable appetite<sup>93</sup> and are more likely to develop obesity.<sup>94</sup> This finding is also consistent with the fact that short sleepers have higher energy intakes than regular sleepers do.<sup>95–97</sup> Nevertheless, bumetanide treatment had no significant effect on food intake under our experimental conditions.

As a potential therapeutic approach for sleep disturbance in DS by NKCC1 inhibition, we used bumetanide because it is an FDA-approved drug that is able to rescue learning and memory deficits in Ts65Dn mice,<sup>17</sup> and it is being tested to rescue cognitive impairment in people with DS (EudraCT Number: 2015-005780-16). A possible limitation of bumetanide treatment for sleep disturbances is its inconvenient diuretic effect (which may impair sleep duration) and the possible ionic imbalance caused by chronic bumetanide administration (if not well compensated by a balanced diet and nutritional supplements).<sup>98,99</sup> Our main claim is, however, that bumetanide rescues sleep quality, as indicated by the NREM power spectra, which has been demonstrated to be key in cognitive improvement, more than the mere sleep duration, in a recent independent study.<sup>65</sup> Moreover, inhibiting GABAergic neurotransmission through a GABA<sub>A</sub> receptor antagonist increases NREM sleep and reduces wake duration in Ts65Dn mice, with no effect on the power spectral density of sleep. This suggests that the regulation of sleep duration may be linked to GABA<sub>A</sub> receptor activity, whereas that of sleep spectral content to GABA<sub>A</sub> receptor-driven Cl<sup>−</sup> current polarity.<sup>100</sup> On the other hand, the use of diuretics can improve breathing in people with OSA by preventing the fluid retention and accumulation responsible for upper airway collapse.<sup>101</sup> Thus, bumetanide treatment could also represent a potential therapy to ameliorate OSA in people with DS.

A valid alternative to avoid bumetanide shortcomings may be the growing arsenal of newly developed molecules that act via selective inhibition of NKCC1 or activation of the neuronal Cl exporter KCC2 and are devoid of diuretic effects.<sup>20,23,102</sup> Some of these new drugs are subject to ongoing evaluations of safety, tolerability, and pharmacokinetics. In contrast to bumetanide, which induces very strong diuresis, these new nondiuretic drugs

would also allow to increase the dosage of NKCC1-inhibiting drugs to optimal levels, thus potentially allowing higher levels of sleep pattern rescue than the only partial rescue that we found here in Ts65Dn mice.

Anyhow, bumetanide has been already proposed as a potential treatment for a total of 30 diverse diseases other than DS, as tested in diverse clinical trials, patient case studies, and preclinical animal models.<sup>22,103,104</sup> Many of these disorders (i.e., autism, Rett syndrome, fragile X syndrome, schizophrenia, traumatic brain injury, epilepsy, Alzheimer disease, and Parkinson disease)<sup>105–108</sup> have also been associated with sleep disturbances. Thus, the proposed potential therapy with bumetanide aimed at rescuing their specific core symptoms could at the same time also ameliorate their associated sleep disorders, which is analogous to the results we described here on the rescue of DS sleep disturbances by NKCC1 inhibition.

In conclusion, our data describe a role for impaired Cl<sup>−</sup> homeostasis in sleep deficits in a mouse model of DS and indicate a therapeutic strategy based on NKCC1 inhibition by an FDA-approved drug ready for repurposing to simultaneously treat sleep and cognitive impairments. This finding holds promise for clinical translation. Given that sleep disorders are often a comorbidity of other brain diseases and that impaired Cl homeostasis and GABA<sub>A</sub>ergic transmission are common in several brain disorders, our translational approach may also be useful for rescuing sleep impairments in these other brain disorders.

### Limitations of the study

Our study revealed significant findings on the beneficial effect of chronic oral bumetanide treatment in Ts65Dn mice, suggesting that impaired Cl homeostasis is associated with sleep disturbances and demonstrating the selective efficacy of bumetanide in improving sleep quality and EEG information content, although with limitations. First, we did not analyze sex differences because we used only male offspring, because major sex differences have not been reported yet in DS. Second, we did not analyze gamma rhythms in our study because our EEG/EMG recording system did not have sufficient sampling frequency or insulation from high-frequency environmental noise to achieve clean gamma power density extraction. Third, bumetanide is an FDA-approved diuretic because it also acts on the NKCC2 transporter in the kidney, besides on NKCC1 in the brain. The diuretic effect of bumetanide in the treatment of sleep abnormalities in DS is particularly inconvenient because it may lead to sleep interruption for the urgency to urinate. A valid alternative to avoid bumetanide shortcomings may be the growing arsenal of newly developed molecules that act via selective inhibition of NKCC1 or activation of the neuronal Cl exporter KCC2 and are devoid of diuretic effects.<sup>20</sup>

### RESOURCE AVAILABILITY

#### Lead contact

Further information required to reanalyze the data reported in this work should be directed to and will be fulfilled by the lead contact, Laura Cancedda (laura.cancedda@iit.it).

#### Material availability

This study did not generate new unique reagents.

### Data and code availability

- The original raw EEG/EMG dataset has been deposited in the IIT Dataverse repository, IIT's local instance of Dataverse, originally developed and used by Harvard University for FAIR data sharing. The data are publicly available as of the date of publication at this link: <https://doi.org/10.48557/PSA7KY>.
- All the code used for entropy/complexity analysis of EEG data generated during this study has been deposited in GitHub and freely available at this link: [https://arthurpessa.github.io/ordpy/\\_build/html/index.html](https://arthurpessa.github.io/ordpy/_build/html/index.html).
- Any additional information required to re-analyze the data reported in this article is available from the [lead contact](#) upon request.

### ACKNOWLEDGMENTS

The authors wish to thank the IIT animal facility staff for their valuable work. This work was partially funded by the European Research Council (ERC) under the European Union's Horizon 2020 research and innovation program (Grant Agreement No. 725563 to L.C.), Telethon Foundation (TCP15021 to L.C.), and Angelini Foundation (168(A)MD21320 to L.C. and V.T.).

### AUTHOR CONTRIBUTIONS

M.B. carried out experiments on mice, analyzed the data, and contributed to the manuscript. M.F. carried out the surgeries and analyzed the EEG/EMG experiments data. G.C. prepared the figures and wrote the manuscript. M.P. supervised and contributed to EEG/EMG experiments. R.B., N.M., and F.M. performed the information theory analysis of EEG signals and contributed to the related figure. V.T. and L.C. conceived the study, designed and supervised the experiments, and wrote the manuscript. All authors read and revised the manuscript.

### DECLARATION OF INTERESTS

L.C. is named as co-inventor on granted patent US 9822368, EP 3083959, JP 6490077; IT 10201900004929; and US11427836. L.C. is also named as co-inventor on the patent applications WO 2018/189225 and PA102109IT101. L.C. is founder and scientific advisor at IAMA therapeutics S.r.l.

### STAR★METHODS

Detailed methods are provided in the online version of this paper and include the following:

- [KEY RESOURCES TABLE](#)
- [EXPERIMENTAL MODEL AND STUDY PARTICIPANT DETAILS](#)
  - Ethics approval declaration
  - Mouse colony
- [METHOD DETAILS](#)
  - Drug treatment and experimental timeline
  - Surgery
  - *In vivo* electrophysiology
  - Deprivation of sleep (SD)
  - Information theory quantifiers and analysis of *in vivo* electrophysiology data
  - Activity assessment
  - Food-intake assessment
- [QUANTIFICATION AND STATISTICAL ANALYSIS](#)

### SUPPLEMENTAL INFORMATION

Supplemental information can be found online at <https://doi.org/10.1016/j.isci.2025.112220>.

Received: September 16, 2024

Revised: December 10, 2024

Accepted: March 11, 2025

Published: March 13, 2025

## REFERENCES

- Dierssen, M. (2012). Down syndrome: The brain in trisomic mode. *Nat. Rev. Neurosci.* **13**, 844–858.
- Stores, R.J. (2019). Sleep problems in adults with Down syndrome and their family carers. *J. Appl. Res. Intellect. Disabil.* **32**, 831–840.
- Maris, M., Verhulst, S., Wojciechowski, M., Van de Heyning, P., and Boudewyns, A. (2017). Outcome of adenotonsillectomy in children with Down syndrome and obstructive sleep apnoea. *Arch. Dis. Child.* **102**, 331–336.
- Long, S., Ding, R., Wang, J., Yu, Y., Lu, J., and Yao, D. (2021). Sleep Quality and Electroencephalogram Delta Power. *Front. Neurosci.* **15**, 803507.
- Grubar, J.C., Gigli, G.L., Colognola, R.M., Ferri, R., Musumeci, S.A., and Bergonzi, P. (1986). Sleep patterns of Down's syndrome children: Effects of butocamide hydrogen succinate (BAHS) administration. *Psychopharmacology* **90**, 119–122.
- Diomed, M., Curatolo, P., Scalise, A., Placidi, F., Caretto, F., and Gigli, G.L. (1999). Sleep abnormalities in mentally retarded autistic subjects: Down's syndrome with mental retardation and normal subjects. *Brain Dev.* **21**, 548–553.
- Levanon, A., Tarasiuk, A., and Tal, A. (1999). Sleep characteristics in children with Down syndrome. *J. Pediatr.* **134**, 755–760.
- Clausen, J., Sersen, E.A., and Lidsky, A. (1977). Sleep patterns in mental retardation: Down's syndrome. *Electroencephalogr. Clin. Neurophysiol.* **43**, 183–191.
- Sibarani, C.R., Walter, L.M., Davey, M.J., Nixon, G.M., and Horne, R.S.C. (2022). Sleep-disordered breathing and sleep macro- and micro-architecture in children with Down syndrome. *Pediatr. Res.* **91**, 1248–1256.
- Hamburg, S., Bush, D., Strydom, A., and Startin, C.M. (2021). Comparison of resting-state EEG between adults with Down syndrome and typically developing controls. *J. Neurodev. Disord.* **13**, 1–11.
- Levenga, J., Peterson, D.J., Cain, P., and Hoeffler, C.A. (2018). Sleep Behavior and EEG Oscillations in Aged Dp(16)1Yey/+ Mice: A Down Syndrome Model. *Neuroscience* **376**, 117–126.
- Colas, D., Valletta, J.S., Takimoto-Kimura, R., Nishino, S., Fujiki, N., Mobley, W.C., and Mignot, E. (2008). Sleep and EEG features in genetic models of Down syndrome. *Neurobiol. Dis.* **30**, 1–7.
- Heise, I., Fisher, S.P., Banks, G.T., Wells, S., Peirson, S.N., Foster, R.G., and Nolan, P.M. (2015). Sleep-like behavior and 24-h rhythm disruption in the Tc1 mouse model of Down syndrome. *Gene Brain Behav.* **14**, 209–216.
- Stenberg, D. (2007). Neuroanatomy and neurochemistry of sleep. *Cell. Mol. Life Sci.* **64**, 1187–1204.
- Morgan, P.T., Pace-Schott, E.F., Mason, G.F., Forselius, E., Fasula, M., Valentine, G.W., and Sanacora, G. (2012). Cortical GABA Levels in Primary Insomnia. *Sleep* **35**, 807–814.
- Alfonsa, H., Burman, R.J., Brodersen, P.J.N., Newey, S.E., Mahfooz, K., Yamagata, T., Panayi, M.C., Bannerman, D.M., Vyazovskiy, V.V., and Akerman, C.J. (2023). Intracellular chloride regulation mediates local sleep pressure in the cortex. *Nat. Neurosci.* **26**, 64–78. <https://doi.org/10.1038/s41593-022-01214-2>.
- Deidda, G., Allegra, M., Cerri, C., Naskar, S., Bony, G., Zunino, G., Bozzi, Y., Caleo, M., and Cancedda, L. (2015). Early depolarizing GABA controls critical-period plasticity in the rat visual cortex. *Nat. Neurosci.* **18**, 87–96.
- Contestabile, A., Magara, S., and Cancedda, L. (2017). The GABAergic Hypothesis for Cognitive Disabilities in Down Syndrome. *Front. Cell. Neurosci.* **11**, 54.
- Parrini, M., Naskar, S., Alberti, M., Colombi, I., Morelli, G., Rocchi, A., Nanni, M., Piccardi, F., Charles, S., Ronzitti, G., et al. (2021). Restoring neuronal chloride homeostasis with anti-NKCC1 gene therapy rescues cognitive deficits in a mouse model of Down syndrome. *Mol. Ther.* **29**, 3072–3092.
- Savardi, A., Borgogno, M., Narducci, R., La Sala, G., Ortega, J.A., Summa, M., Armirotti, A., Bertorelli, R., Contestabile, A., De Vivo, M., and Cancedda, L. (2020). Discovery of a Small Molecule Drug Candidate for Selective NKCC1 Inhibition in Brain Disorders. *Chem* **6**, 2073–2096.
- Borgogno, M., Savardi, A., Manigrasso, J., Turci, A., Portoli, C., Ottonello, G., Bertozzi, S.M., Armirotti, A., Contestabile, A., Cancedda, L., and De Vivo, M. (2021). Design, Synthesis, In Vitro and In Vivo Characterization of Selective NKCC1 Inhibitors for the Treatment of Core Symptoms in Down Syndrome. *J. Med. Chem.* **64**, 10203–10229.
- Savardi, A., Borgogno, M., De Vivo, M., and Cancedda, L. (2021). Pharmacological tools to target NKCC1 in brain disorders. *Trends Pharmacol. Sci.* **42**, 1009–1034.
- Savardi, A., Patricelli Malizia, A., De Vivo, M., Cancedda, L., and Borgogno, M. (2023). Preclinical Development of the Na-K-2Cl Co-transporter-1 (NKCC1) Inhibitor ARN23746 for the Treatment of Neurodevelopmental Disorders. *ACS Pharmacol. Transl. Sci.* **6**, 1–11.
- Portoli, C., Ruiz Munevar, M.J., De Vivo, M., and Cancedda, L. (2021). Cation-coupled chloride cotransporters: chemical insights and disease implications. *Trends Chem.* **3**, 832–849.
- Tang, X., Jaenisch, R., and Sur, M. (2021). The role of GABAergic signaling in neurodevelopmental disorders. *Nat. Rev. Neurosci.* **22**, 290–307.
- Shelton, A.R., and Malow, B. (2021). Neurodevelopmental Disorders Commonly Presenting with Sleep Disturbances. *Neurotherapeutics* **18**, 156–169.
- Hauw, J.-J., Hausser-Hauw, C., De Girolami, U., Hasboun, D., and Seilhean, D. (2011). Neuropathology of Sleep Disorders: A Review. *J. Neuropathol. Exp. Neurol.* **70**, 243–252.
- Tyzio, R., Nardou, R., Ferrari, D.C., Tsintsadze, T., Shahrokhi, A., Eftekhari, S., Khalilov, I., Tsintsadze, V., Bouchoud, C., Chazal, G., et al. (2014). Oxytocin-Mediated GABA Inhibition During Delivery Attenuates Autism Pathogenesis in Rodent Offspring. *Science* **343**, 675–679.
- Ito, J., Roy, S., Liu, Y., Cao, Y., Fletcher, M., Lu, L., Boughter, J.D., Grün, S., and Heck, D.H. (2014). Whisker barrel cortex delta oscillations and gamma power in the awake mouse are linked to respiration. *Nat. Commun.* **5**, 3572.
- Tort, A.B.L., Ponsel, S., Jessberger, J., Yanovsky, Y., Brankač, J., and Draguhn, A. (2018). Parallel detection of theta and respiration-coupled oscillations throughout the mouse brain. *Sci. Rep.* **8**, 6432.
- Leung, L.S. (1984). Theta rhythm during REM sleep and waking: correlations between power, phase and frequency. *Electroencephalogr. Clin. Neurophysiol.* **58**, 553–564.
- Bandt, C., and Pompe, B. (2002). Permutation Entropy: A Natural Complexity Measure for Time Series. *Phys. Rev. Lett.* **88**, 174102.
- Rosso, O.A., Larrondo, H.A., Martin, M.T., Plastino, A., and Fuentes, M.A. (2007). Distinguishing Noise from Chaos. *Phys. Rev. Lett.* **99**, 154102.
- Rosso, O.A., and Masoller, C. (2009). Detecting and quantifying stochastic and coherence resonances via information-theory complexity measurements. *Phys. Rev. E* **79**, 040106.
- Guisande, N., and Montani, F. (2024). Rényi entropy-complexity causality space: a novel neurocomputational tool for detecting scale-free features in EEG/IEEG data. *Front. Comput. Neurosci.* **18**, 1342985.
- Baravalle, R., Rosso, O.A., and Montani, F. (2018). Rhythmic activities of the brain: Quantifying the high complexity of beta and gamma oscillations during visuomotor tasks. *Chaos* **28**, 075513.
- Escorihuela, R.M., Fernández-Teruel, A., Vallina, I.F., Baamonde, C., Lumbrales, M.A., Dierssen, M., Tobeña, A., and Flórez, J. (1995). A behavioral assessment of Ts65Dn mice: a putative Down syndrome model. *Neurosci. Lett.* **199**, 143–146.
- Morris-Rosendahl, D.J., and Crocq, M.A. (2020). Neurodevelopmental disorders—the history and future of a diagnostic concept. *Dialogues Clin. Neurosci.* **22**, 65–72.
- Parmeggiani, P.L. (1987). Interaction Between Sleep and Thermoregulation: An Aspect of the Control of Behavioral States. *Sleep* **10**, 426–435.

40. Miyazaki, S., Liu, C.-Y., and Hayashi, Y. (2017). Sleep in vertebrate and invertebrate animals, and insights into the function and evolution of sleep. *Neurosci. Res.* 118, 3–12.
41. Wintler, T., Schoch, H., Frank, M.G., and Peixoto, L. (2020). Sleep, brain development, and autism spectrum disorders: Insights from animal models. *J. Neurosci. Res.* 98, 1137–1149.
42. Deidda, G., Parrini, M., Naskar, S., Bozarth, I.F., Contestabile, A., and Cancedda, L. (2015). Reversing excitatory GABA A R signaling restores synaptic plasticity and memory in a mouse model of Down syndrome - SI. *Nat. Med.* 21, 318–326.
43. Lau, Z.J., Pham, T., Chen, S.H.A., and Makowski, D. (2022). Brain entropy, fractal dimensions and predictability: A review of complexity measures for EEG in healthy and neuropsychiatric populations. *Eur. J. Neurosci.* 56, 5047–5069.
44. Volk, C., and Huber, R. (2015). Sleep to grow smart. *Arch. Ital. Biol.* 153, 99–109. <https://doi.org/10.12871/000398292015235>.
45. Śmigielka-Kuzia, J., Sobaniec, W., Kułsak, W., and Boćkowski, L. (2009). Clinical and EEG features of epilepsy in children and adolescents in down syndrome. *J. Child Neurol.* 24, 416–420.
46. Buzsáki, G. (2002). Theta Oscillations in the Hippocampus. *Neuron* 33, 1–16.
47. Uygun, D.S., and Basheer, R. (2022). Circuits and components of delta wave regulation. *Brain Res. Bull.* 188, 223–232.
48. Jantzie, L.L., Hu, M.Y., Park, H.K., Jackson, M.C., Yu, J., Maxwell, J.R., and Jensen, F.E. (2015). Chloride cotransporter NKCC1 inhibitor bumetanide protects against white matter injury in a rodent model of periventricular leukomalacia. *Pediatr. Res.* 77, 554–562.
49. MacAulay, N., Keep, R.F., and Zeuthen, T. (2022). Cerebrospinal fluid production by the choroid plexus: a century of barrier research revisited. *Fluids Barriers CNS* 19, 26.
50. Untiet, V. (2024). Astrocytic chloride regulates brain function in health and disease. *Cell Calcium* 118, 102855.
51. De Vivo, L., and Bellesi, M. (2019). The role of sleep and wakefulness in myelin plasticity. *Glia* 67, 2142–2152.
52. Yamazaki, Y., Abe, Y., Fujii, S., and Tanaka, K.F. (2021). Oligodendrocytic Na<sup>+</sup>-K<sup>+</sup>-Cl<sup>-</sup> co-transporter 1 activity facilitates axonal conduction and restores plasticity in the adult mouse brain. *Nat. Commun.* 12, 5146.
53. Deng, S., Gan, L., Liu, C., Xu, T., Zhou, S., Guo, Y., Zhang, Z., Yang, G.Y., Tian, H., and Tang, Y. (2023). Roles of Ependymal Cells in the Physiology and Pathology of the Central Nervous System. *Aging Dis.* 14, 468–483. <https://doi.org/10.14336/AD.2022.0826-1>.
54. Ingiosi, A.M., and Frank, M.G. (2023). Goodnight, astrocyte: waking up to astroglial mechanisms in sleep. *FEBS J.* 290, 2553–2564.
55. Kharod, S.C., Kang, S.K., and Kadam, S.D. (2019). Off-Label Use of Bumetanide for Brain Disorders: An Overview. *Front. Neurosci.* 13, 310.
56. Santos, R.A., Costa, L.H., Linhares, R.C., Pradella-Hallinan, M., Coelho, F.M.S., and Oliveira, G.d.P. (2022). Sleep disorders in Down syndrome: a systematic review. *Arq. Neuropsiquiatr.* 80, 424–443.
57. Stickgold, R., and Walker, M.P. (2005). Sleep and Memory: The Ongoing Debate. *Sleep* 28, 1225–1227.
58. Dang-Vu, T.T., Desseilles, M., Peigneux, P., and Maquet, P. (2006). A role for sleep in brain plasticity. *Pediatr. Rehabil.* 9, 98–118.
59. Berres, S., and Erdfelder, E. (2021). The sleep benefit in episodic memory: An integrative review and a meta-analysis. *Psychol. Bull.* 147, 1309–1353.
60. Wilckens, K. A., Ferrarelli, F., Walker, M. P., and Buysse, D. J. (2018). Slow-wave activity enhancement to improve cognition. *Trends Neurosci.* 41, 470–482.
61. Reeves, R.H., Irving, N.G., Moran, T.H., Wohn, A., Kitt, C., Sisodia, S.S., Schmidt, C., Bronson, R.T., and Davisson, M.T. (1995). A mouse model for Down syndrome exhibits learning and behaviour deficits. *Nat. Genet.* 11, 177–184.
62. Fernandez, F., Morishita, W., Zuniga, E., Nguyen, J., Blank, M., Malenka, R.C., and Garner, C.C. (2007). Pharmacotherapy for cognitive impairment in a mouse model of Down syndrome. *Nat. Neurosci.* 10, 411–413.
63. Trois, M. S., Capone, G. T., Lutz, J. A., Melendres, M. C., Schwartz, A. R., Collop, N. A., and Marcus, C. L. (2009). Obstructive sleep apnea in adults with Down syndrome. *J. Clin. Sleep Med.* 5, 317–323.
64. Costa, A.C.S., Scott-McKean, J.J., and Stasko, M.R. (2008). Acute Injections of the NMDA Receptor Antagonist Memantine Rescue Performance Deficits of the Ts65Dn Mouse Model of Down Syndrome on a Fear Conditioning Test. *Neuropsychopharmacology* 33, 1624–1632.
65. Pittaras, E., Colas, D., Chuluun, B., Allocca, G., and Heller, C. (2022). Enhancing sleep after training improves memory in down syndrome model mice. *Sleep* 45, zsab247.
66. Chen, C.-W., Kwok, Y.T., Cheng, Y.T., Huang, Y.S., Kuo, T.B.J., Wu, C.H., Du, P.J., Yang, A.C., and Yang, C.C.H. (2023). Reduced slow-wave activity and autonomic dysfunction during sleep precede cognitive deficits in Alzheimer's disease transgenic mice. *Sci. Rep.* 13, 11231.
67. Schreiner, S.J., Imbach, L.L., Valko, P.O., Maric, A., Maqkaj, R., Werth, E., Baumann, C.R., and Baumann-Vogel, H. (2021). Reduced Regional NREM Sleep Slow-Wave Activity Is Associated With Cognitive Impairment in Parkinson Disease. *Front. Neurol.* 12, 618101.
68. Backus, A.R., Schoffelen, J.-M., Szebenyi, S., Hanslmayr, S., and Doeller, C.F. (2016). Hippocampal-Prefrontal Theta Oscillations Support Memory Integration. *Curr. Biol.* 26, 450–457.
69. Scheeringa, R., Bastiaansen, M.C.M., Petersson, K.M., Oostenveld, R., Norris, D.G., and Hagoort, P. (2008). Frontal theta EEG activity correlates negatively with the default mode network in resting state. *Int. J. Psychophysiol.* 67, 242–251.
70. Nigbur, R., Ivanova, G., and Stürmer, B. (2011). Theta power as a marker for cognitive interference. *Clin. Neurophysiol.* 122, 2185–2194.
71. Cohen, M.X. (2014). A neural microcircuit for cognitive conflict detection and signaling. *Trends Neurosci.* 37, 480–490.
72. Huang, P., Xiang, X., Chen, X., and Li, H. (2020). Somatostatin Neurons Govern Theta Oscillations Induced by Salient Visual Signals. *Cell Rep.* 33, 108415.
73. Musaeus, C.S., Engedal, K., Høgh, P., Jelic, V., Mørup, M., Naik, M., Oek-sengaard, A.R., Snaedal, J., Wahlund, L.O., Waldemar, G., and Andersen, B.B. (2018). EEG Theta Power Is an Early Marker of Cognitive Decline in Dementia due to Alzheimer's Disease. *J. Alzheimers Dis.* 64, 1359–1371.
74. Zawisłak-Fomagiel, K., Ledwoń, D., Bugdol, M., Romaniszyn-Kania, P., Małeck, A., Gorzkowska, A., and Mitas, A.W. (2023). The Increase of Theta Power and Decrease of Alpha/Theta Ratio as a Manifestation of Cognitive Impairment in Parkinson's Disease. *J. Clin. Med.* 12, 1569.
75. Montgomery, S.M., Sirota, A., and Buzsáki, G. (2008). Theta and Gamma Coordination of Hippocampal Networks during Waking and Rapid Eye Movement Sleep. *J. Neurosci.* 28, 6731–6741.
76. Hasselmo, M.E., and Stern, C.E. (2014). Theta rhythm and the encoding and retrieval of space and time. *Neuroimage* 85, 656–666.
77. Boyce, R., Glasgow, S.D., Williams, S., and Adamantidis, A. (2016). Causal evidence for the role of REM sleep theta rhythm in contextual memory consolidation. *Science* 352, 812–816.
78. Heller, H.C.1., Freeburn, A.2., Finn, D.P.2,3., and Munn, R.G.K. (2020). 2, 3. Disordered phasic relationships between hippocampal place cells, theta, and gamma rhythms in the Ts65Dn mouse model of Down Syndrome. Preprint at bioRxiv. <https://doi.org/10.1101/2020.09.17.3014321>.
79. Grosmark, A.D., Mizuseki, K., Pastalkova, E., Diba, K., and Buzsáki, G. (2012). REM Sleep Reorganizes Hippocampal Excitability. *Neuron* 75, 1001–1007.
80. Chen, M., Wang, J., Jiang, J., Zheng, X., Justice, N.J., Wang, K., Ran, X., Li, Y., Huo, Q., Zhang, J., et al. (2017). APP modulates KCC2 expression and function in hippocampal GABAergic inhibition. *Elife* 6, e20142.



81. Xu, W., Tan, C.-C., Zou, J.-J., Cao, X.-P., and Tan, L. (2020). Sleep problems and risk of all-cause cognitive decline or dementia: an updated systematic review and meta-analysis. *J. Neurol. Neurosurg. Psychiatry* **97**, 236–244.
82. Pistollato, F., Sumalla Cano, S., Elio, I., Masias Vergara, M., Giampieri, F., and Battino, M. (2016). Associations between Sleep, Cortisol Regulation, and Diet: Possible Implications for the Risk of Alzheimer Disease. *Adv. Nutr.* **7**, 679–689.
83. Thomas, J., Ooms, S.J., Mentink, L.J., Booij, J., Olde Rikkert, M.G.M., Overeem, S., Kessels, R.P.C., and Claassen, J.A.H.R. (2020). Effects of long-term sleep disruption on cognitive function and brain amyloid- $\beta$  burden: a case-control study. *Alzheimers Res. Ther.* **12**, 101.
84. Ekstein, S., Glick, B., Weill, M., Kay, B., and Berger, I. (2011). Down syndrome and attention-deficit/hyperactivity disorder (ADHD). *J. Child Neurol.* **26**, 1290–1295.
85. Vacca, R.A., Bawari, S., Valenti, D., Tewari, D., Nabavi, S.F., Shirooie, S., Sah, A.N., Volpicella, M., Braidy, N., and Nabavi, S.M. (2019). Down syndrome: Neurobiological alterations and therapeutic targets. *Neurosci. Biobehav. Rev.* **98**, 234–255.
86. Howells, F.M., Stein, D.J., and Russell, V.A. (2012). Synergistic tonic and phasic activity of the locus coeruleus norepinephrine (LC-NE) arousal system is required for optimal attentional performance. *Metab. Brain Dis.* **27**, 267–274.
87. Castelnovo, A., Turner, K., Rossi, A., Galbiati, A., Gagliardi, A., Proserpio, P., Nobili, L., Terzaghi, M., Manni, R., Ferini Strambi, L., et al. (2021). Behavioural and emotional profiles of children and adolescents with disorders of arousal. *J. Sleep Res.* **30**, e13188.
88. Chervin, R.D., Dillon, J.E., Bassetti, C., Ganoczy, D.A., and Pituch, K.J. (1997). Symptoms of Sleep Disorders, Inattention, and Hyperactivity in Children. *Sleep* **20**, 1185–1192.
89. Yoon, S.Y.R., Jain, U., and Shapiro, C. (2012). Sleep in attention-deficit/hyperactivity disorder in children and adults: Past, present, and future. *Sleep Med. Rev.* **16**, 371–388.
90. Roberts, D.M., Schade, M.M., Mathew, G.M., Gartenberg, D., and Buxton, O.M. (2020). Detecting sleep using heart rate and motion data from multisensor consumer-grade wearables, relative to wrist actigraphy and polysomnography. *Sleep* **43**, zsa045.
91. Harding, E.C., Franks, N.P., and Wisden, W. (2020). Sleep and thermoregulation. *Curr. Opin. Physiol.* **15**, 7–13.
92. Dierssen, M., Fructuoso, M., Martínez De Lagrán, M., Perluigi, M., and Barone, E. (2020). Down Syndrome Is a Metabolic Disease: Altered Insulin Signaling Mediates Peripheral and Brain Dysfunctions. *Front. Neurosci.* **14**, 670.
93. Weijerman, M.E., and De Winter, J.P. (2010). Clinical practice: The care of children with Down syndrome. *Eur. J. Pediatr.* **169**, 1445–1452.
94. Bertapelli, F., Pitetti, K., Agiovlasis, S., and Guerra-Junior, G. (2016). Overweight and obesity in children and adolescents with Down syndrome—prevalence, determinants, consequences, and interventions: A literature review. *Res. Dev. Disabil.* **57**, 181–192.
95. Imaki, M., Hatanaka, Y., Ogawa, Y., Yoshida, Y., and Tanada, S. (2002). An Epidemiological Study on Relationship between the Hours of Sleep and Life Style Factors in Japanese Factory Workers. *J. Physiol. Anthropol. Appl. Hum. Sci.* **21**, 115–120.
96. Weiss, A., Xu, F., Storfer-Isser, A., Thomas, A., levers-Landis, C.E., and Redline, S. (2010). The Association of Sleep Duration with Adolescents' Fat and Carbohydrate Consumption. *Sleep* **33**, 1201–1209.
97. Dashti, H.S., Scheer, F.A., Jacques, P.F., Lamon-Fava, S., and Ordovás, J.M. (2015). Short Sleep Duration and Dietary Intake: Epidemiologic Evidence, Mechanisms, and Health Implications. *Adv. Nutr.* **6**, 648–659.
98. Ward, A., and Heel, R.C. (1984). Bumetanide A Review of its Pharmacodynamic and Pharmacokinetic Properties and Therapeutic Use. *Drugs* **28**, 426–464.
99. Lemonnier, E., Degrez, C., Phelep, M., Tyzio, R., Josse, F., Grandgeorge, M., Hadjikhani, N., and Ben-Ari, Y. (2012). A randomised controlled trial of bumetanide in the treatment of autism in children. *Transl. Psychiatry* **2**, e202.
100. Pittaras, E.C., Artal, J.M., Ajibola, G., Allocca, G., Bennett, M., Camargo, A., Carpio, A., Gessner, N., Hinton, M., Pizzitola, R., et al. (2024). Short term GABA antagonist treatment improves long term sleep quality, memory, and decision-making in a Down syndrome mouse model. *Sleep*, zsa0300. <https://doi.org/10.1093/sleep/zsa0300>.
101. Fiori, C.Z., Martinez, D., Montanari, C.C., Lopez, P., Camargo, R., Sezerá, L., Gonçalves, S.C., and Fuchs, F.D. (2018). Diuretic or sodium-restricted diet for obstructive sleep apnea—a randomized trial. *Sleep* **41**, zsy016.
102. Zhang, J., Bhuiyan, M.I.H., Zhang, T., Karimy, J.K., Wu, Z., Fiesler, V.M., Zhang, J., Huang, H., Hasan, M.N., Skrzypiec, A.E., et al. (2020). Modulation of brain cation-Cl<sup>−</sup> cotransport via the SPAK kinase inhibitor ZT-1a. *Nat. Commun.* **11**, 78.
103. Damier, P., Degos, B., Castelnovo, G., Anheim, M., Benatru, I., Carrière, N., Colin, O., Defebvre, L., Deverdal, M., Eusebio, A., et al. (2024). A Double-Blind, Randomized, Placebo-Controlled Trial of Bumetanide in Parkinson's Disease. *Mov. Disord.* **39**, 618–622. <https://doi.org/10.1002/mds.29726>.
104. Ben-Ari, Y. (2017). NKCC1 Chloride Importer Antagonists Attenuate Many Neurological and Psychiatric Disorders. *Trends Neurosci.* **40**, 536–554.
105. Lajoie, A.C., Lafontaine, A.-L., and Kaminska, M. (2021). The Spectrum of Sleep Disorders in Parkinson Disease. *Chest* **159**, 818–827.
106. Mattai, A.A., Tossell, J., Greenstein, D.K., Addington, A., Clasen, L.S., Gornick, M.C., Seal, J., Inoff-Germain, G., Gochman, P.A., Lenane, M., et al. (2006). Sleep disturbances in childhood-onset schizophrenia. *Schizophr. Res.* **86**, 123–129.
107. Gau, S.S.F., Kessler, R.C., Tseng, W.L., Wu, Y.Y., Chiu, Y.N., Yeh, C.B., and Hwu, H.G. (2007). Association Between Sleep Problems and Symptoms of Attention-Deficit/Hyperactivity Disorder in Young Adults. *Sleep* **30**, 195–201.
108. Al-Biltagi, M.A. (2014). Childhood epilepsy and sleep. *World J. Clin. Pediatr.* **3**, 45–53.
109. Pessa, A.A., and Ribeiro, H.V. (2021). ordpy: A Python package for data analysis with permutation entropy and ordinal network methods. *Chaos* **31**. <https://doi.org/10.48550/arXiv.2102.06786>.
110. Duchon, A., Raveau, M., Chevalier, C., Nalesso, V., Sharp, A.J., and Hérault, Y. (2011). Identification of the translocation breakpoints in the Ts65Dn and Ts1Cje mouse lines: relevance for modeling down syndrome. *Mamm. Genome* **22**, 674–684.
111. Pace, M., Camilo, M.R., Seiler, A., Duss, S.B., Mathis, J., Manconi, M., and Bassetti, C.L. (2018). Rapid eye movements sleep as a predictor of functional outcome after stroke: a translational study. *Sleep* **41**, zsy138.



## STAR★METHODS

### KEY RESOURCES TABLE

REAGENT or RESOURCE	SOURCE	IDENTIFIER
<b>Chemicals, peptides, and recombinant proteins</b>		
Dimethyl Sulfoxide (DMSO)	Sigma–Aldrich	Cat# 276855
Bicuculline methiodide	Sigma–Aldrich	Cat# 14343
IsoVet (isoflurane 1000 mg/mL)	Piramal Critical Care Italia S.p.A.	N.A.
Sterile saline solution (500 mL) NaCl 0.9%	B Braun	Cat# 3570410
Paracetamol (Tempra; 100 mg/mL)	Taisho Pharmaceuticals Inc.	N.A.
Enrofloxacin (Baytril; 25 mg/mL)	Elanco Italia S.p.A.	N.A.
<b>Deposited data</b>		
IIT Dataverse	IIT	<a href="https://doi.org/10.48557/PSA7KY">https://doi.org/10.48557/PSA7KY</a>
<b>Experimental models: Organisms/strains</b>		
Mouse:B6EiC3Sn a/A-Ts(1716)65Dn/J	The Jackson Laboratory	Cat# JAX:001924, RRID:IMSR_JAX:001924
<b>Software and algorithms</b>		
GraphPad PRISM	GraphPad Software Inc.	<a href="https://www.graphpad.com/scientificsoftware/prism/">https://www.graphpad.com/scientificsoftware/prism/</a> ; RRID:SCR_002798
Sleep Sign	Kissei Comtec Co Ltd.	<a href="http://www.sleepsign.com/">http://www.sleepsign.com/</a> ; RRID:SCR_018200
Dataquest A.R.T.	DSI, Harvard Bioscience Ltd.	<a href="https://www.datasci.com/products/software/dataquest-art">https://www.datasci.com/products/software/dataquest-art</a>
MATLAB	MathWorks	<a href="https://it.mathworks.com/products/MATLAB.html">https://it.mathworks.com/products/MATLAB.html</a> ; RRID:SCR_001622
Python	Python Software Foundation	<a href="https://www.python.org/">https://www.python.org/</a> ; RRID:SCR_008394
ordpy: A Python package for data analysis with permutation entropy and ordinal network methods.	Pessa and Ribeiro <sup>109</sup>	<a href="https://arthurpessa.github.io/ordpy/_build/html/index.html">https://arthurpessa.github.io/ordpy/_build/html/index.html</a>
<b>Other</b>		
TL11M2-F20-EET	DSI, Harvard Bioscience Ltd.	N.A.
Model 900 Small Animal Stereotaxic Instrument	David Kopf Instruments	Cat# 900

### EXPERIMENTAL MODEL AND STUDY PARTICIPANT DETAILS

#### Ethics approval declaration

All animal procedures were approved by IIT licensing in compliance with the Italian Ministry of Health (D.Lgs 26/2014) and EU guidelines (Directive 2010/63/EU; study approval number 807/2018-PR, protocol number 176AA.149; study approval number 568/2019-PR, protocol number 176AA.62). A veterinarian was employed to maintain the health and comfort of the animals.

#### Mouse colony

The mice were housed in filtered cages in a temperature-controlled room with a 12:12 h dark/light cycle and *ad libitum* access to water and food. All efforts were made to minimize animal suffering and to use the lowest possible number of animals required to produce statistically relevant results, according to the “3Rs concept.” In this study, we used Ts65Dn mice maintained in their original genetic background<sup>61</sup> by crossing (more than 40 times) Ts65Dn females with C57BL/6JEi × C3SnHeSnJ (B6EiC3) F1 males (Jackson Laboratories). Ts65Dn mice were genotyped using PCR, as previously described.<sup>110</sup>

Male offspring, naive for drug treatment or tests and aged 3–4 months, were used for the experiments. We chose to use only male offspring in accordance with extensive previous literature<sup>18</sup> and because major sex differences are not reported in DS.<sup>1</sup>

## METHOD DETAILS

### Drug treatment and experimental timeline

Ts65Dn and WT littermates were randomly assigned to vehicle groups (0.15% DMSO in drinking water) or bumetanide groups (Merck Life Sciences; 3-(Butylamino)-4-phenoxy-5-sulfamoylbenzoic acid 2 mg/kg body weight in drinking water, as described previously<sup>28</sup> and as previously demonstrated to be beneficial for the Ts65Dn mouse model of DS<sup>23</sup> and (starting 3 days after surgery for electrode implantation) treated chronically for 4–5 days before and during 1 day of EEG and EMG baseline recordings and further 1 day during EEG and EMG upon sleep deprivation (SD).

### Surgery

The mice were anesthetized with 2–2.5% isoflurane in oxygen and placed in a stereotaxic frame (David Kopf Instruments, Tujunga, CA). To assess the sleep–wake cycle, the mice were surgically implanted with a telemetric transmitter (volume, 1.9 cm<sup>3</sup>; total weight, 3.9 g; TL11M2-F20-EET; DSI, St. Paul, MN, USA) connected to electrodes for continuous EEG/EMG recordings. A wireless EEG transmitter/receiver, which also contains a sensor to detect body temperature, was subcutaneously implanted. Specifically, EEG wire electrodes were implanted into the frontal cortex (coordinates: 2 mm posterior to the bregma and 2 mm lateral to the midline in the right parietal skull) and the parietal cortex (coordinates: 3 mm anterior to the lambda and 2 mm lateral to the midline in the right frontal skull). EMG signals were recorded by two stainless steel wires inserted bilaterally into the neck muscles. One screw placed in the cerebellum was wrapped around the electrode ground. Following surgery, all the animals were administered paracetamol (200 mg/kg; once a day; *per os*; Tempra) or enrofloxacin (10 mg/kg; once a day; subcutaneously; Baytril) for two days. Following recovery, recordings were collected from the telemetry system, which included LFP, EMG, general locomotor activity, and body temperature data from freely moving animals in their home cages.

### *In vivo* electrophysiology

Cortical EEG/EMG signals were recorded via Dataquest A.R.T. (Data Science International; Lassi et al., 2012). The signals were digitized at a sampling rate of 500 Hz with a filter cutoff of 50 Hz. EEG signals were filtered at 0.3 Hz (low-pass filter) and 0.1 kHz (high-pass filter). The polysomnographic recordings were visually scored offline via SleepSign software (Kissei Comtec Co. Ltd., Japan) with a 4-s epoch window to identify wakefulness, non-REM or REM sleep stages, as previously described.<sup>111</sup> Scoring was performed by an observer blinded to the experimental groups. Specifically, wake, non-REM and REM states were scored when characteristic EEG/EMG activity occupied 75% of the epochs. EEG epochs determined to have artifacts (interference caused by mouse scratching, movement, eating, or drinking) were excluded from the analysis. Artifacts were noted in <5–8% of all the recordings used for analysis. The percentage of time spent in total sleep, non-REM and REM sleep out of the total recording time was determined. The amount of time spent in each stage was established by counting the types of epochs (wake, NREM or REM) and averaging over 2-h periods (bins). The spectral characteristics of the EEGs were further analyzed. The EEG power densities of the delta (0.5–5 Hz) and theta (5–9 Hz) frequencies in non-REM and REM sleep were computed for all conditions investigated. To exclude variability because of the implantation, the power density of each animal was normalized to the power density of the last 4 h of the light period of the 24-h recording. The temperature was recorded at a sampling rate of 5 Hz within the range of 34°C–41°C and averaged over 2-h periods.

### Deprivation of sleep (SD)

For sleep deprivation (6 h), the mice were kept awake by the experimenter's intervention. A brush was used by the experimenter any time that the animal assumed a sleeping posture. Moreover, various objects were introduced into the mouse cage to stimulate curiosity, resulting in sleep deprivation with the least amount of stress.

### Information theory quantifiers and analysis of *in vivo* electrophysiology data

Brain signals can be studied as complex systems, which are difficult to predict because of their intricate structure. However, we can use theoretical approaches on information to describe brain signals. Indeed, the properties of EEG signals are quantified through the informational content of such systems. Time-domain analysis of entropy and complexity is particularly suited for detecting nonlinear dynamics in brain signals. Entropy in the time domain quantifies the unpredictability and randomness of brain activity as it unfolds over time, whereas complexity captures how structured or organized these temporal changes are. These measures can reveal important nonlinear, transient, and time-dependent phenomena that are often overlooked or averaged out using spectral (frequency-domain) analysis. As such, time-domain analysis provides a richer, complementary view of brain dynamics.

A time series is a sequence of data collected over time, such as recorded brain signals.<sup>32–35</sup> The Bandt and Pompe methodology enables the quantification of the probability distributions associated with different patterns within a time series, facilitating an analysis of the temporal structure and complexity inherent in the data. This is done by estimating the histogram of trend patterns (how the signal changes, i.e., how the time series increases or decreases from a time point to the next) and thus considers how the amplitude at a given time is related to the signal's contiguous ones.

In this formalism, the size of the window used to consider the trend between a given time and the contiguity of a signal depends on the embedding dimension (D) and the time lag ( $\tau$ ). The embedding dimension refers to the size of the time window, whereas the time

lag refers to the spacing between considered points. In that sense, it is said to capture and quantify the causality of the signal. To achieve this, we use an embedding dimension of  $D=6$  and a time lag of  $\tau = 1$ , as in the original work of Band and Pompe.<sup>32,33</sup> The complexity and entropy were subsequently computed using these PDFs. Importantly, the Band and Pompe approach to measuring complexity and entropy is particularly useful for separating chaotic signals from noisy signals.<sup>33</sup>

In this context, entropy (H) is estimated to describe the level of disorder within the system. For a system such as the EEG signal, entropy quantifies how unpredictable or disorganized the system is. On the other hand, complexity (C) measures the structure within the system. It is zero when there is no structure or when the system is in a state of maximum disorder. This can be understood by estimating the distance between the EEG system's band and Pompe PDF for a given neurophysiological condition and the equiprobable state using a statistical measure called Jensen–Shannon divergence that quantifies the difference between these distributions. Thus, complexity is associated with the underlying structures or patterns that govern the dynamics of a system.<sup>32–35</sup>

Therefore, time-domain analysis of entropy and complexity is particularly effective for identifying the nonlinear dynamics inherent in brain signals. The code used for the entropy and complexity analysis presented in this work is available online.<sup>34</sup>

### Activity assessment

Changes in locomotor activity levels (quantified in “units” proprietary to the DSI telemetry system) in the home cage were collected via an additional telemetry channel of the telemetric transmitter (volume, 1.9 cm<sup>3</sup>; total weight, 3.9 g; TL11M2-F20-EET; DSI, Saint Paul, MN, USA). Daily averages of activity levels were calculated by averaging the total hourly activity across each session.

### Food-intake assessment

The food intake index was calculated across 24 h at baseline as the ratio of food intake to mouse weight.

## QUANTIFICATION AND STATISTICAL ANALYSIS

The statistical tests were performed with MATLAB, Python and GraphPad Prism 8.3. two-way ANOVA with repeated measures (factors of group  $\times$  time) was used for the statistical analysis of the 2-h averaged time-course changes in the percentage of each sleep stage (wake, NREM and REM sleep), delta power, theta power and body temperature between the two genotypes. The statistical analysis of the cumulative amount of wake, NREM, and REM sleep over the dark and light periods among the groups at baseline, after SD and vehicle vs. treatment was performed with one-way ANOVA followed by all-pairwise Šidák's *post hoc* test. An unpaired *t* test was used to compare differences in the sleep stages and in the delta and theta power during the first 4 h of rebound after SD between the two genotypes. Two-way mixed analyses of variance (ANOVAs; Genotype  $\times$  Treatment) were conducted on temperature, activity, and food intake to compare WT with Ts mice across light and dark phases. When equal variance assumptions were not valid, statistical significance was evaluated via ANOVA with the Welch correction followed by all pairwise Dunnett's *post hoc* tests.

For all the ANOVA tests, the threshold *p* values were # < 0.05, ## < 0.01, ### < 0.001, and #### < 0.0001, and for all the *post hoc* tests, the threshold *p* values were \* < 0.05, \*\* < 0.01, \*\*\* < 0.001, and \*\*\*\* < 0.0001. These variables represented the probability of committing type I error, which rejected the null hypothesis when it was in fact true. Outliers were excluded only from the final pool of data by Grubbs' test (GraphPad, alpha = 0.05), which was iteratively performed until no outliers were found.